

Prediction of sound pressure level for a dual-stage hydromechanical transmission

Alarico Macor^a , Antonio Rossetti^b  and Martina Scamperle^a 

^aDepartment of Engineering and Management, University of Padua, Vicenza, Italy; ^bConstruction Technologies Institute, National Research Council, Corso Stati Uniti, Padova, Italy

ABSTRACT

Hydromechanical continuously variable transmissions are frequently used in high power applications, including agricultural vehicles, buses and heavy vehicles. These offer several operative advantages such as improved driving comfort, better operational management and less fuel consumption if appropriately managed. However, the acoustic impact that they generate in the environment, which should be checked in the early stages of the project, is often neglected. This paper studies the noise emitted by a drive train for urban buses, which comprises a natural gas engine and a hydromechanical input coupled dual-stage transmission. The aim of this study is the evaluation of the noise emitted by the transmission compared with that emitted by the engine, which is considered the main noise source in the vehicle. The study was carried out by means of a model of the entire vehicle that was implemented in an Amesim environment. The mechanical model was integrated with the acoustic models of the engine and of the transmission. The results show that the transmission, despite its two hydraulic machines, produces a sound pressure level lower by about 2 to 15 dBA than that of the engine, whereas its contribution to the total pressure level does not exceed 1 dBA.

ARTICLE HISTORY

Received 22 June 2015
Accepted 10 November 2015

KEYWORDS

Sound pressure level;
CVT noise; dual-stage;
hydromechanical
transmission; input
coupled

1. Introduction

Continuously variable transmissions (CVTs) are particularly appreciated for the possibility offered of producing an infinite number of transmission ratios for comfort, performance and economy of operation. However, they have some limitations such as a lower load capacity and less than excellent overall efficiency that limit its use compared with other types of more competitive transmission (e.g. manual transmissions).

To overcome these limitations, the Power-Split technology was conceived, which combines the CVT with a planetary gearbox. The power generated by the engine upstream of the system is separated into two branches: a purely mechanical one with high efficiency, and a variable one whose efficiency depends on the type of CVT considered. The powers downstream of the planetary gearbox are then reunited and reconverted into mechanical power, with a certain total efficiency.

The Power-Split configuration that actually achieves the best compromise between performance and costs seems to be a hydromechanical transmission, whose variable branch is the hydrostatic transmission. Hydromechanical transmissions have been classified in the literature into four main types (Kress 1968): input coupled (IC), output

coupled (OC), hydraulic differential and compound. The first two differ from each other in the positioning of the planetary gear unit: in IC type, it is positioned to the wheel side; in OC type, it is connected directly to the engine. The last two configurations have a complex layout. Another interesting complex layout is the dual-stage configuration (Blake *et al.* 2006), which is the object of this study.

The efficiency of a hydromechanical transmission reaches its maximum values near a particular operating point, the full mechanical point FMP, in which the power is transmitted only through the mechanical path (Kress 1968, Casoli *et al.* 2007).

The vehicle speed is regulated by acting on the displacement of the two hydraulic machines. In this way, the engine speed is no longer linked to the wheel speed and it can be freely managed, for example in minimum consumption conditions.

The problem with the design of this type of transmission has been approached in the literature by Blake *et al.* (2006) and Casoli *et al.* (2007), who also supply the design relationships of the hydraulic and mechanical components. An innovative approach to transmission design is based on an optimisation problem. Macor and Rossetti (2011) designed a transmission, maximising its efficiency along the speed range of the vehicle; Rossetti and Macor (2013)

applied multi-objective optimisation to maximise efficiency while minimising transmission volume.

Even more appropriate for high power vehicles are IC and OC transmissions and their complex configuration, called IC Dual-Stage and OC Compound, respectively (Blake *et al.* 2006). They achieve wider speed range compared with IC and OC layouts, thanks to a mechanical gear shift.

The hydraulic units inside the CVT create structural vibrations because of the internal pressure variation and the flow pulsations that are distributed along the hydraulic line (Klop *et al.* 2009). The producers of hydrostatic transmissions are aware of the necessity of improving the acoustic characteristics in the early stages of the design. This is because of two technological requirements: the compliance of regulations in terms of sound emissions, which impose a severe limitation on every type of apparatus, and the improvement of the acoustic performance imposed by market requirements, because a high noise level in new products is increasingly less tolerated. Consequently, technical research has focused on the investigation of noise sources (Klop and Ivantysynova 2011) and on the reduction of the noise problem in hydraulic machines (Kumar Seeniraj *et al.* 2011, Kumar Seeniraj and Ivantysynova 2011). On the other hand, the engine manufacturers have made progress in reducing the noise of their products.

Dual-stage transmissions, and more generally Power-Split transmissions (Renius and Rainer 2005), have been mainly designed for agricultural use; therefore, they have never been subjected to the issue of noise. In fact, their widespread use has never created great inconvenience.

Recent studies (Macor and Rossetti 2013) have shown that a dual-stage transmission could be suitable in applications where frequent stops and starts occur, such as urban buses. Accordingly, the noise problem can be decisive. For this reason, more of the literature is focused on the investigation of noise sources (Klop and Ivantysynova 2011) and reduction of the noise problem in hydraulic machines (Kumar Seeniraj *et al.* 2011).

Therefore, the subject of the present paper is the noise emissions of a dual-stage transmission installed on an urban bus. In particular, the study aims to understand whether a dual-stage transmission generates a significant noise contribution compared with that generated by the engine.

To answer this question without resorting to expensive bench tests, a model of an urban bus was developed by using a simulation environment (AMEsim Software, 2013). The models of the engine and the transmission were integrated with a model for predicting sound emission.

2. Dual-stage hydromechanical transmission

The typical configuration of a dual-stage transmission is shown in Figure 1 (Blake *et al.* 2006). The dual-stage planetary gearbox, a feature from which the entire system takes its name, allows a gear change.

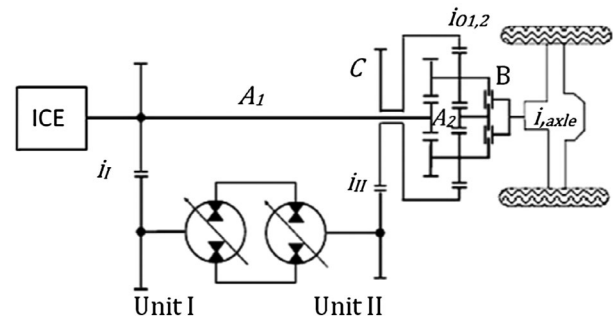


Figure 1. Scheme of IC dual-stage transmission.

Table 1. Main engine and vehicle features for IC dual-stage transmission.

General bus features	
Model	Citelis-12
Constructor	Iveco Irisbus
Number of seats	86
Total weight	12000 [kg]
Total height	3.3 [m]
Total width	2.5 [m]
Total length	12 [m]
Total admissible weight	19845 [kg]
Maximum speed	68 [km/h]
Type of tyres	275/70 R22.5
General engine features	
Model	Iveco Cursor 8
Fuel	CNG
Motor type	6 cylinders in line
Maximum power	190 [kW]
Max rotational speed	2050 [rpm]
Maximum torque	1076 (at 1100 rpm) [Nm]

Table 2. Main design variables of the transmission.

Design transmission variables	
n_{ICE}	1500 [rpm]
r_{tire}	0.448 [m]
p_{max}	450 [bar]
T_{wheel}	20600 [Nm]
$\tau_{mech,1}$	0.5
$\tau_{mech,2}$	2
τ_{shift}	1
i_{axle}	10.143
$i_{0,1}$	-1
$i_{0,2}$	-3
i_I	0.58
i_{II}	0.581
V_I, V_{II}	125 [cc]
$n_{I,max}, n_{II,max}$	2600 [rpm]

This is performed by the clutch when the rotational speed of the planet carrier B and the sun gear A2 are synchronous.

Unlike the traditional IC transmissions, for dual-stage systems the FMP happens twice, once preceding and once following the gear shift. Consequently, the high efficiency operating zone occurs twice.

The design of the transmission has been performed by following the guidelines suggested by Blake *et al.* (2006). The main technical data of the vehicle and the engine are reported in Table 1, and the results of the transmission design are summarised in Table 2.

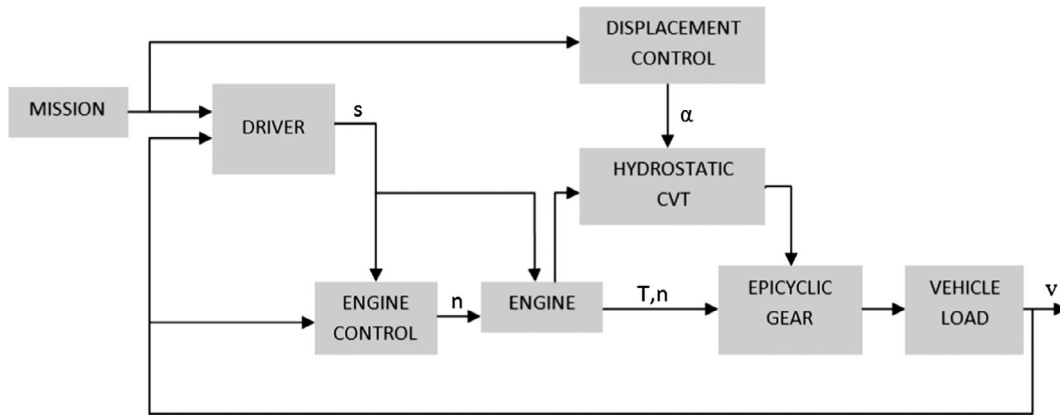


Figure 2. Block scheme of the vehicle test.

2.1. Simulation model of the vehicle

The block scheme of the vehicle model is shown in Figure 2.

Since the transmission is kinematically separated from the engine, two different control systems provide for the engine management and for the transmission management.

In the block simulating the driver, the vehicle speed is compared with the mission speed, to give as output a command s for the accelerator or for the brake. The accelerator command s enters the control strategy block to manage the engine according to a predetermined criterion. In this way, the engine supplies the required power to the transmission.

The transmission is equipped with a control system that receives the vehicle speed signal, and acts on the displacement partialisation of the two hydraulic machines in order to impose the desired speed.

From the perspective of efficiency and noise emission, the most important parts of the model are the engine and the hydraulic CVT. They were shaped as described in the following paragraphs.

2.1.1. Engine

The engine model is an ideal torque generator, whose driving torque was a function of the rotational speed and the accelerator position. The fuel consumption was calculated on the basis of the actual load and rotational speed. The speed-torque characteristic of the engine and the fuel consumption data were derived from experimental measures reported in the literature by De Simio *et al.* (2010). The normalised engine map and the experimental points are reported in Figure 3. In order to take into account the engine dynamics, the engine inertia and a first-order delay on the accelerator signal have been added to the torque generator model, as shown in Figure 4.

2.1.2. Hydromechanical transmission

The model of the hydraulic CVT (Figure 5) is based on a standard scheme for a hydrostatic transmission, with

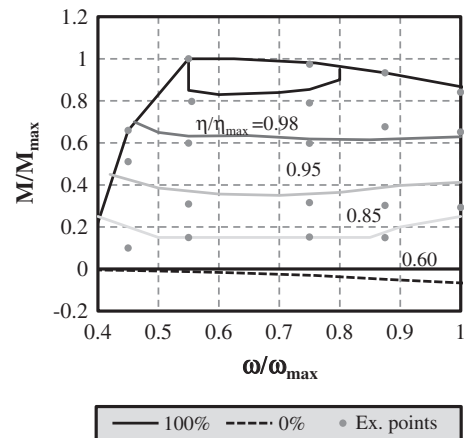


Figure 3. Normalised efficiency map of the engine.

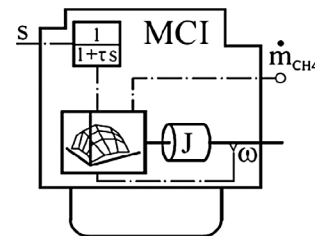


Figure 4. Dynamic model of the engine.

relief valves, boost pump, counter pressure and flushing valves. The hydraulic units were modelled by applying to an ideal unit the main loss sources (Figure 6): friction by means of a brake (C), and leakage by means of the orifices d .

In order to consider the influence of the operating conditions on the unit losses, both the friction torque of the brake C and the diameter of the orifices (d_{flow} , d_{lk}) were expressed as polynomial functions of the rotational speed, the pressure difference and the actual to maximum displacement ratio. The coefficients of the loss models were fitted to the experimental data supplied by a manufacturer. The overall performance of the hydraulic CVT is reported in Figure 7 for different operating conditions.

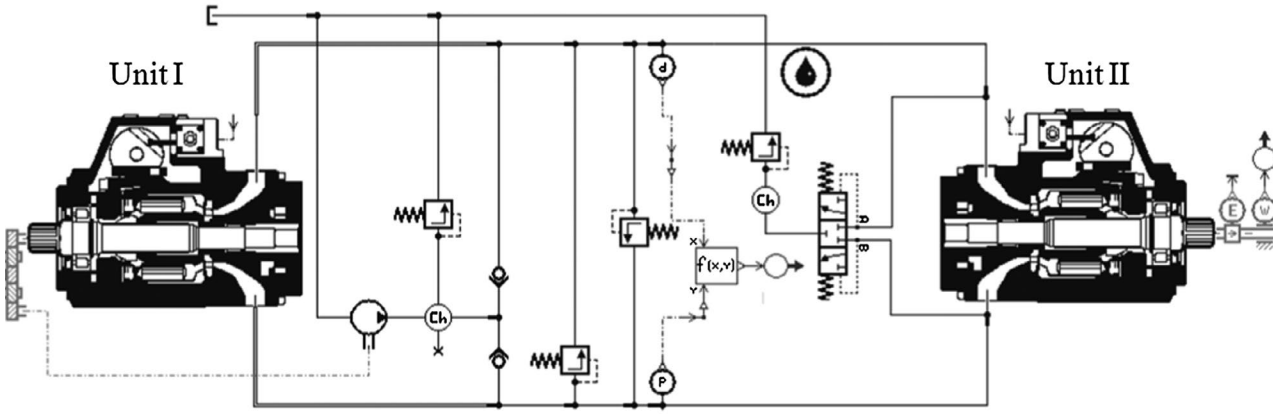


Figure 5. Scheme of hydrostatic CVT transmission.

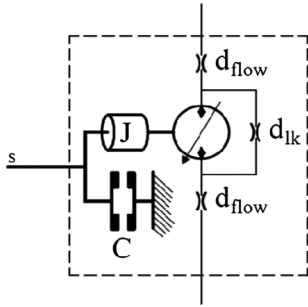


Figure 6. Real pump functional scheme.

Each gear pair of the model, both ordinary pairs and pairs belonging to the epicyclical gear, was assumed to have a constant efficiency $\eta_{\text{gear}} = 0.980$. The vehicle loads, i.e. the aerodynamic friction and the rolling friction, were modelled according to:

$F_a = 0.5 c_d v^2 A_f$ and $F_r = k_r Mg$; where for the vehicle mass, drag coefficient, frontal area, and rolling resistance coefficient the following values were respectively assumed: $M = 14,900$ kg, $c_d = 1.18$, $A_f = 7$ m², $k_r = 0.008$.

The engine control strategy adopted in this model is the simplest one, known as *Speed Envelope* (Pfiffner and Guzzella 2001). It operates on the basis of the vehicle speed and accelerator position, without any optimisation procedure.

3. Sound pressure level prediction models

The sound pressure contributions of the engine and the hydrostatic transmission are considered as predominant. The sound emission of other components, such as the planetary gearbox, the mechanical gears, the hydraulic elements, etc., proved to be very low and therefore negligible.

3.1. Internal combustion engine noise emissions

The noise generated by an engine is a function of several design variables. It would be a hard task to take all of them into account. A simplified predictive model for high power engines (Blair and Spechko 1972, Bies

and Hansen 1988) is therefore applied, which considers three most important contributions to noise emissions: engine exhaust system noise, engine housing noise and air intake system noise. This is a good reference model for noise forecasts, but it could overestimate the noise values because it is dated. The new generation engines are quieter and more isolated than the old-generation ones.

The sound power level generated by the engine exhaust system with a muffler can be estimated using the expression (1):

$$L_{W,ex} = 108 + 10 \log_{10} P + K - (l_{ex}/1.2) \quad (1)$$

where the K parameter indicates the reduction factor owed to the presence of the turbocharger. The l_{EX} parameter indicates the length of the exhaust pipe and P indicates the instantaneous gas engine power.

The noise emission related to engine housing is not univocally determined from only one relation, because it is a function both of the engine speed and of the structure of the system. The sound power level is obtained by using the expression (2):

$$L_{W,h} = 93 + 10 \log_{10} P + J_1 + J_2 + J_3 + J_4 \quad (2)$$

where P indicates the instantaneous engine power and the parameters J_1 , J_2 , and J_3 are respectively the correction terms in function of the engine rotational speed (3), of the fuel type (4) and the arrangement of cylinders (5):

$$\begin{cases} J_1 = -5 & n \leq 600 \text{ rpm} \\ J_1 = -2 & 600 \text{ rpm} < n \leq 1500 \text{ rpm} \\ J_1 = 0 & n > 1500 \text{ rpm} \end{cases} \quad (3)$$

$$\begin{cases} J_2 = 0 & \text{diesel engine or dual fuel engine: diesel/CNG} \\ J_2 = -3 & \text{CNG engine} \end{cases} \quad (4)$$

$$\begin{cases} J_3 = 0 & \text{cylinder arrangement: in - line} \\ J_3 = -1 & \text{cylinder arrangement: V - type o radial - type} \end{cases} \quad (5)$$

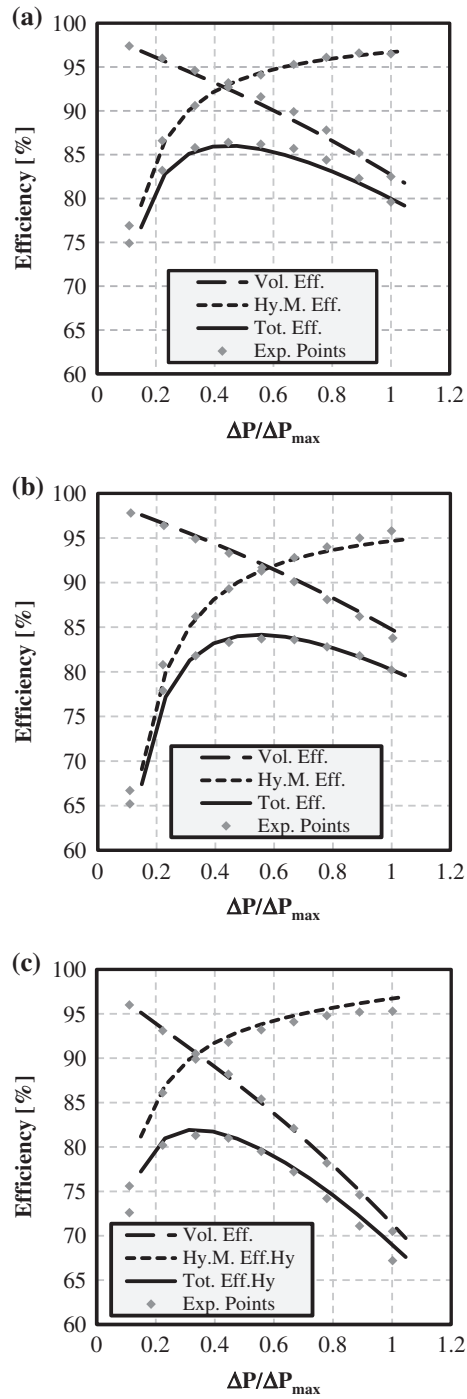


Figure 7. Efficiency of the hydraulic CVT for different operating conditions. Comparison between model (lines) and experimental data (dots): (a) $n_1 = 2000$ rpm, $\alpha_1 = 1$, $\alpha_{II} = 1$; (b) $n_1 = 3000$ rpm, $\alpha_1 = 1$, $\alpha_{II} = 1$; (c) $n_1 = 2000$ rpm, $\alpha_1 = 0.5$, $\alpha_{II} = 1$.

In order to obtain the sound power level values filtered through the A-weighting curve, a correction (6) of their total value must be made.

$$\begin{cases} J_4 = -4 & n \leq 600 \text{ rpm} \\ J_4 = -3 & 600 \text{ rpm} < n \leq 1500 \text{ rpm} \\ J_4 = -1 & n > 1500 \text{ rpm} \end{cases} \quad (6)$$

To predict the sound power level for the engine intake air system with the turbocharger, the next relation (7) can be used:

$$L_{W,\text{int}} = 92 + 5 \log_{10} P - l_{\text{int}}/1.8 \quad (7)$$

where l_{int} is the length of the input duct.

To make a comparison between the last expressions and the output result from the hydrostatic noise model, the sound power level must be converted into the sound pressure level. To this end it is possible to calculate the sound pressure level at a certain distance r if we know the sound power level of a point source and its acoustic directional factor Q , using expression (8) for diffuse fields:

$$L_p = L_W + 10 \cdot \log \left(\frac{Q}{4\pi r^2} + \frac{4}{R} \right) \quad (8)$$

The acoustic room constant R is obtained in (9) as we know the total surface S and the acoustic absorption coefficient a_{abs} by using Sabine's law (Moncada Lo Giudice and Santoboni 1995).

$$R = S \cdot a_{\text{abs}} / (1 - a_{\text{abs}}) \quad (9)$$

For an omnidirectional noise power source, placed on a totally reflective hemispheric plane ($Q = 2$), the Equations (8) and (9) can be condensed in the following simplified formula:

$$L_p = L_W - 20 \cdot \log r - 8 \quad (10)$$

When more than one source emits a known sound pressure, the overall sound pressure level can be calculated by means of the relation (11):

$$L_{p,\text{TOT}} = 10 \cdot \log_{10} \sum_{k=1}^N 10^{\frac{L_{p,k}}{10}} \quad (11)$$

which expresses the sum of the individual sound pressure expressed in decibels. The expression (11) will also be used for summing the sound contributions of the gas engine and of the hydrostatic CVT.

3.2. Hydrostatic CVT noise emissions

The literature indicates there are three main noise sources in a hydraulic system (Bies and Hansen 1988): *air-borne noise*, that is the noise transmitted through the air, which is that most easily heard by the human ear; *fluid-borne noise*, generated by an irregular fluid flow and by some pressure oscillations in the hydraulic pipeline; *structure-borne noise*, which is the noise generated by the mechanical and structural elements of the machine.

The authors developed a polynomial formulation of the noise produced by the Hydrostatic-CVT, based on experimental noise data performed by the manufacturer at different operating condition. Phonometric measurements were performed in a hemi-anechoic chamber on two hydraulic axial piston pumps, at an inlet fluid temperature of 50 °C. They relate to the A-weighting curve.

The curves of sound pressure level are shown as a function of hydraulic pressure and rotational speed. In Figure 8(a) and (b) the curves refer to a displacement of 75 cc and a partialisation respectively equal to $\alpha = 100\%$ and 25%. In Figure 8(c) and (d) the curves refer to a displacement of 90 cc and a partialisation respectively equal to $\alpha = 100\%$ and 25%. As can be seen in the graphs, the SPL increases with both the pressure and the rotational speed; it decreases with the displacement of the hydraulic units.

The experimental curves have been interpolated by means of a polynomial equation expressed as a function of pressure, rotational speed, displacement and partialisation of displacement:

$$\text{SPL [dBA]} = f(p, n, V, \alpha) \quad (12)$$

The general form of the equation is the following (13):

$$\text{SPL [dBA]} = An^2 + Bn + C \quad (13)$$

where the coefficients A, B, and C have been obtained through a regression of experimental data and have the form shown in (14):

$$A = a_A \cdot (\alpha V) + b_A \quad B = a_B \cdot (\alpha V) + b_B \quad C = a_C \cdot (\alpha V) + b_C$$

$$a_A = k_A \cdot (p) + \gamma_A \quad a_B = k_B \cdot (p) + \gamma_B \quad a_C = k_C \cdot (p) + \gamma_C$$

$$b_A = k'_A \cdot (p) + \gamma'_A \quad b_B = k'_B \cdot (p) + \gamma'_B \quad b_C = k'_C \cdot (p) + \gamma'_C \quad (14)$$

In Equation (14) the coefficients A, B, and C are expressed as a function of the product of the partialisation and displacement and of the parameters $a_A, b_A, a_B, b_B, a_C, b_C$. These parameters are considered dependent on the hydraulic operative pressure only.

In Figure 9 the curves resulting from the application of the model (dots) are compared with the experimental data (lines) for a displacement of 90 cc and partialisation of $\alpha = 100\%$.

The low-grade polynomial nature of the experimental model allows a good forecast of the noise values even for pressures and rotational speeds outside the ranges shown in Figure 9. The average root mean square error between the experimental data and the prediction of the polynomial model was approximately 0.469 dBA, with a maximum value of 1.14 at 200 bar and 1500 rpm.

4. Simulation and results

Two speed missions were used in the simulations: the trapezoidal mission (Figure 10) and the Manhattan mission (Figure 11) (DieselNet 2014). They are shown along with their characteristic parameters respectively in Tables 3 and 4. The latter simulates the real route for an urban bus with sudden accelerations, deceleration and frequent starts and stops typical of this kind of vehicle,

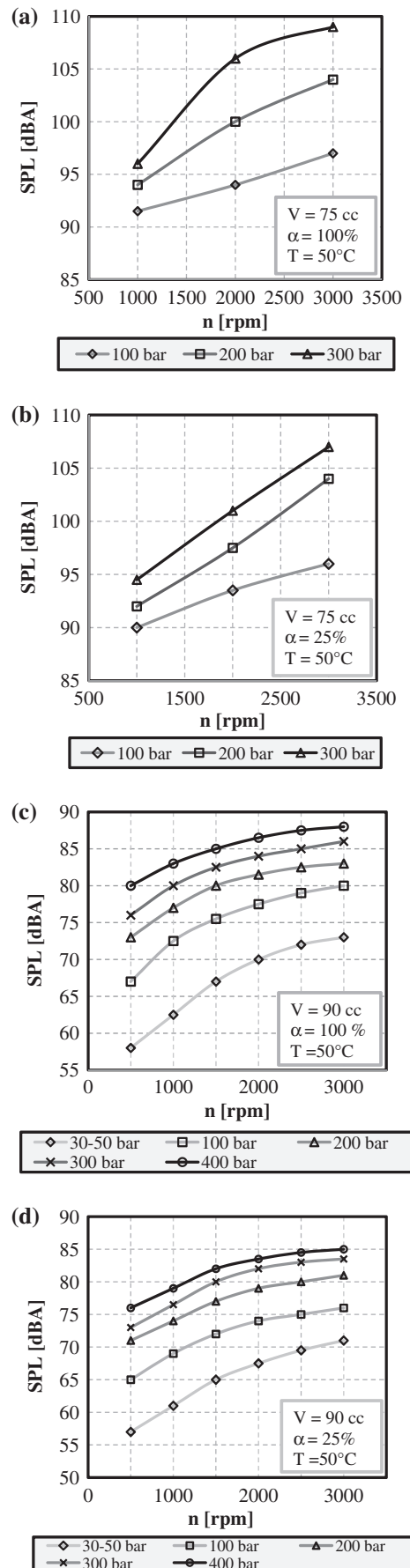


Figure 8. SPL in function of pressure and rotational speed of the hydrostatic unit: (a) $\alpha = 100\%$ and $V = 75$ cc; (b) $\alpha = 25\%$ and $V = 75$ cc (c) $\alpha = 100\%$ and $V = 90$ cc (d) $\alpha = 25\%$ and $V = 90$ cc.

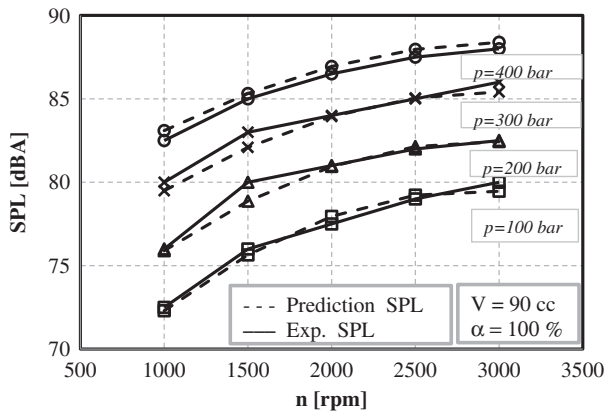


Figure 9. Experimental (lines) and prediction (dots) curves for displacement of 90 cc and partialisation of $\alpha = 100\%$.

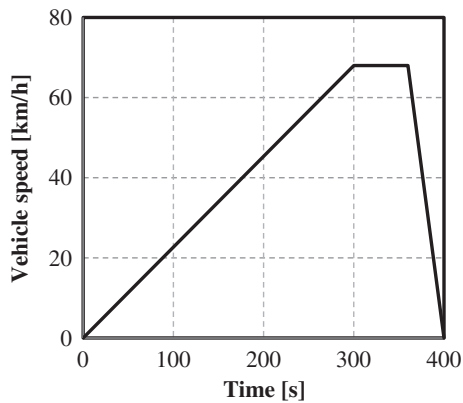


Figure 10. Trapezoidal speed mission.

and the former is used to highlight the relative importance of the noise sources in a simple acceleration-deceleration test.

The sound pressure level of the two hydrostatic units is shown in Figure 12; it has been calculated according to (14). In the section where the vehicle has reached its maximum speed, the SPL keeps a constant level of about 80 dBA for both the hydraulic units. In fact, in this section no quantity affecting the noise varies. In the acceleration section, the sound pressure level is affected

by the variation of the hydraulic pressure (Figure 13(c)). During the gear shift the pressure of Unit I decreases, while that of Unit II increases; this defines the discontinuity in the graph of sound emissions.

The sharp drop in noise emission of the two hydraulic units at the FMPs (at about 48 s and 190 s) is mainly owed to the speed variation for Unit II and the displacement variation for Unit I, as shown in Figure 13(a) and (b).

Initially the circuit works in *negative circulating mode*: the first hydraulic unit works as a motor and the second unit works as a pump. After the FMP the flow is inverted into the CVT and the shift to *power split mode* happens.

In Figure 13 the speed, the displacement and the pressure variation of the hydraulic units are shown. The speed of Unit II is imposed solely by the incoming flow rate, i.e. by the combined action of the speed (Figure 13(a)) and the displacement of the Unit I (Figure 13(b)).

The former slightly increases according to the control strategy of the engine. In the first acceleration phase, and hence with the first gear inserted, the rotational speed of the wheels is imposed by the planet carrier B . When its rotational speed is synchronous with the speed of the sun gear A_2 , the clutches are activated, and the gear shift occurs. Now the sun gear A_2 imposes the motion.

In Figure 14 the trend of the sound pressure level of the gas engine with all its contributions is reported. The trends are similar because the SPL depends mainly on the engine power, as shown by Equations (1), (2) and (7).

The predominant contribution to the sound emission in Figure 14 is the engine housing, which is followed by the exhaust system. This result agrees with what is observed in practice: what creates the noise is the fuel combustion inside the cylinders together with the structural vibration of the engine. During the deceleration, the air intake system's contribution is the most important one. The other sound source in this phase, the braking system, is not considered in this analysis.

The SPLs of the CVT and the engine are shown in Figure 15. They have been calculated by means of Equation (11) as the sum of all the contributions shown

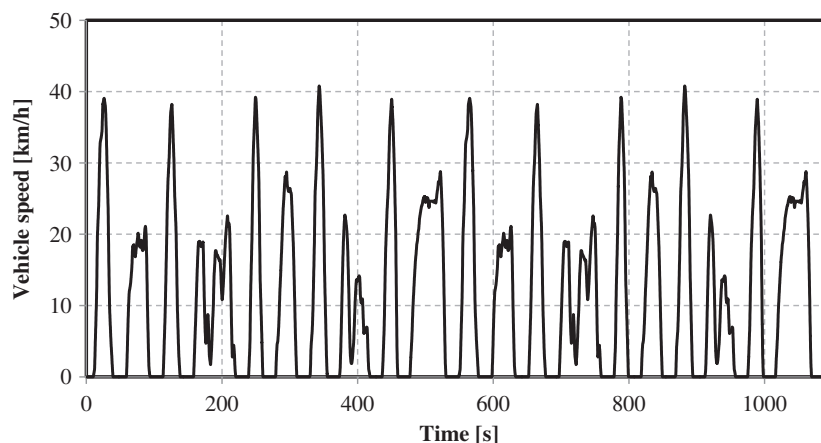


Figure 11. Manhattan speed mission.

Table 3. Characteristic parameters of trapezoidal speed mission.

Duration	400	[s]
Stops time/duration	100	[%]
Total driving distance	4.3	[km]
Maximum speed	68	[km/h]
Time at constant speed	60	[s]
Maximum acceleration	0.063	[m/s ²]
Number of stops per km	0	[-]

Table 4. Characteristic parameters of Manhattan speed mission.

Duration	1089	[s]
Stops time/duration	36	[%]
Total driving distance	3.33	[km]
Maximum speed	40.9	[km/h]
Average speed	11	[km/h]
Average speed without stops	17.17	[km/h]
Maximum acceleration	2.24	[m/s ²]
Number of stops per km	6	[-]

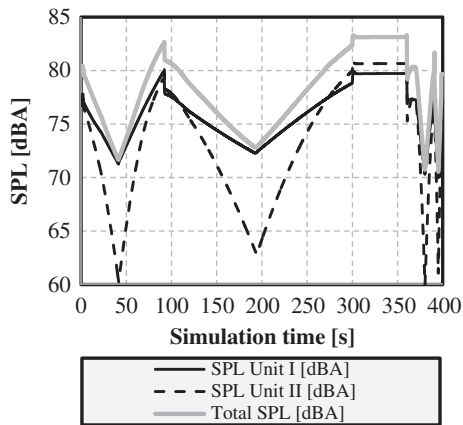


Figure 12. Sound pressure level of the hydraulic units.

in Figure 13. As can be seen, the SPL of the engine is always greater than that of the transmission; the difference is particularly evident at the FMP where it reaches 15 dBA.

The efficiencies of the engine and the CVT are also shown in Figure 15. The efficiencies and the SPL have similar trends. This can be explained by the fact that efficiency and noise depend on the same parameters. For the engine, they mainly depend on the power; for the CVT, they depend on pressure, speed and partialisation.

We can observe that the value of sound pressure level for the gas engine is generally higher than the SPL of the CVT for values that are between 5 and 15 dBA. In the worst case, the SPL of the engine reaches about 90 dBA, vs. the 83 dBA of the transmission. Despite this high value of SPL, the CVT contributes slightly to the SPL of the engine-transmission group. In fact, considering the engine as the main noise source, the CVT contribution becomes equal to 0.8 dBA (Equation (11)).

The overall sound pressure levels for the Manhattan mission are represented in Figure 16. In Figure 17, instead, the first 100 s are zoomed in.

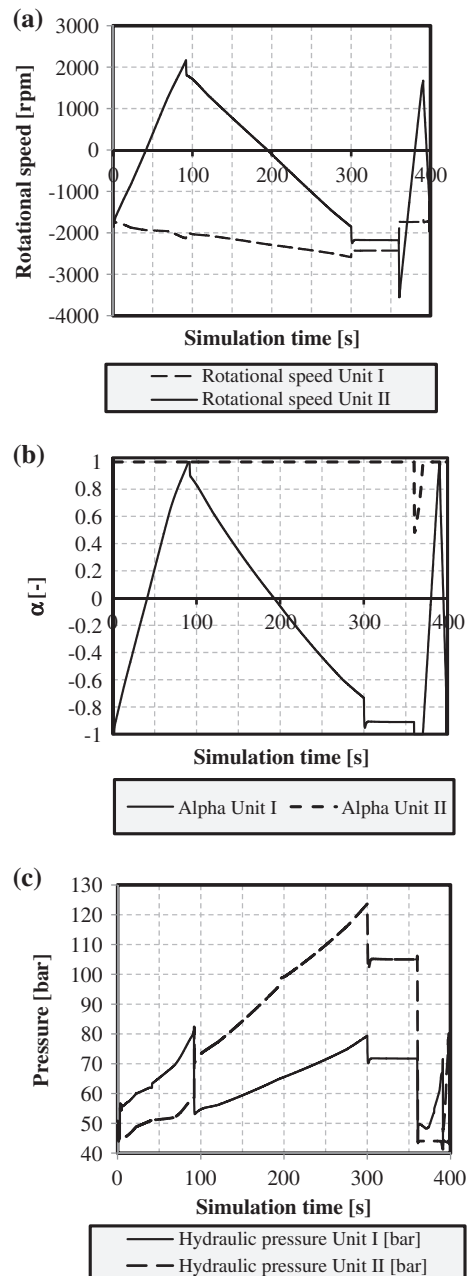


Figure 13. (a) Variation of rotational speed, (b) displacement partialisation and (c) hydraulic pressure of Unit I and Unit II.

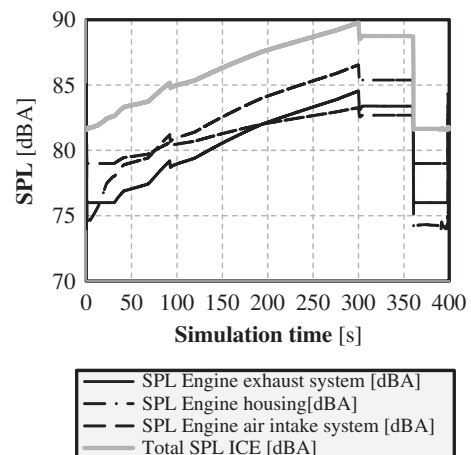


Figure 14. SPL of gas engine with noise contributions.

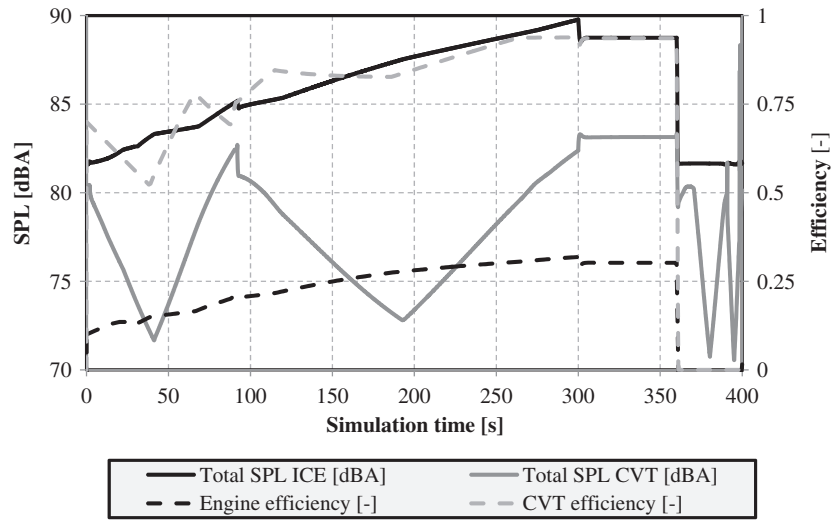


Figure 15. Comparison between the total SPL of gas engine and the total SPL of CVT.

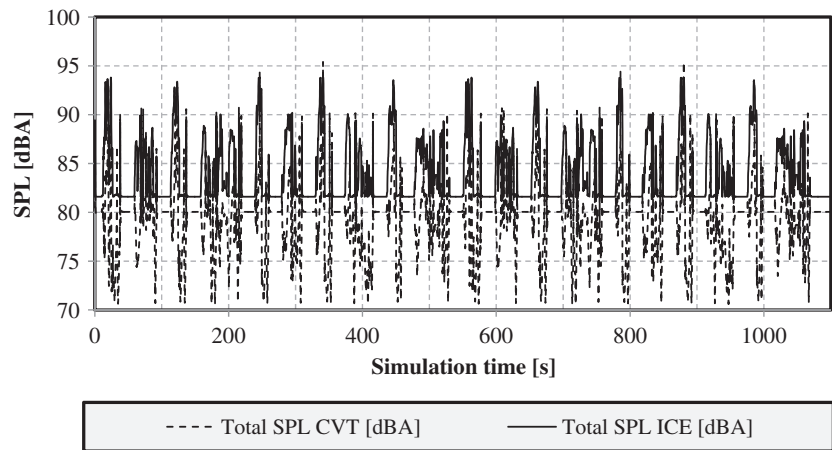


Figure 16. Total SPL for Manhattan speed mission.

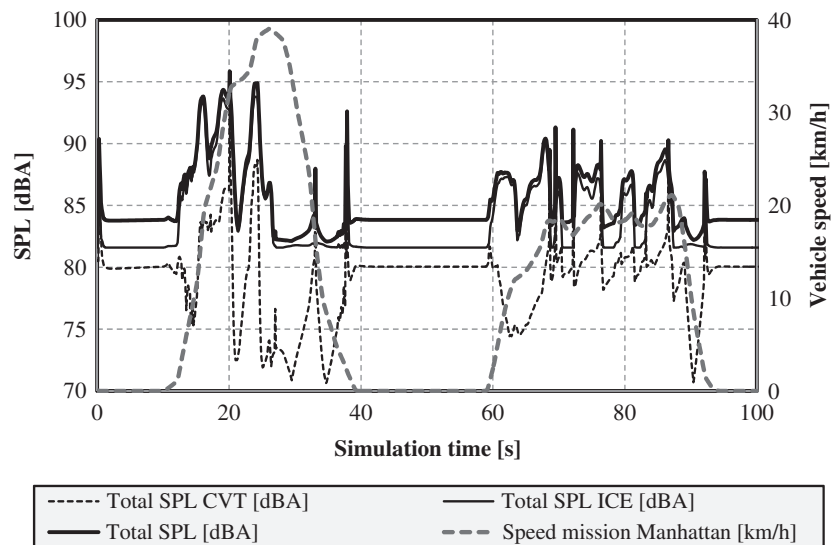


Figure 17. Total SPL for Manhattan speed mission in the first 100 s of simulation.

Even in this mission, the SPL of the engine is always greater than that of the CVT, and the transmission

contribution to noise generation is quite small, as shown in Figure 17.

However, the CVT contribution depends also on the engine type.

For CNG engines, as the present one, showing SPL peaks of 85–90 dBA, the transmission contribution is equal to 0.8–2 dBA, because the transmission peak is 83 dBA. If diesel engines are considered, whose SPL peak values range between 95 and 100 dBA, the transmission contribution drops to 0.1–0.3 dBA.

5. Conclusions

In this work, the noise emitted from a dual-stage hydro-mechanical transmission of a bus has been studied by means of a simulation model. The aim was to assess the relative weight of the noise produced by the DS within the total noise generated by the engine transmission group.

The engine noise was described according to an empirical model taken from the literature; the noise model of the hydromechanical transmission was inferred by means of a linear regression technique applied on experimental data provided by a manufacturer. The output model values may be slightly overestimated because the new generation engines are modern and more acoustically isolated.

The simulation results have shown the following.

The hydraulic pressure is the most important parameter affecting the sound emission of the transmission.

The pressure also influences the gear shift phase where a sensible increment of noise can be observed. During the full mechanical point, a strong decrease of pressure sound level occurs, because of the annulment of the displacement value of the first hydraulic unit.

Regarding the gas engine, the main contribution of the emission is the housing, followed by the exhaust system; less important is the effect owed to the air intake system.

Although the transmission is equipped with two hydraulic machines, it contributes slightly to the total noise of the engine transmission group.

Nomenclature

Acronyms

CNG	Combustion natural gas
CVT	Continuously variable transmission
FMP	Full mechanical point
IC	Input coupled
ICE	Internal combustion engine
OC	Output coupled
SPL	Sound pressure level, [dBA]

Symbols

α	Displacement partialisation, [-]
a_{abs}	Acoustic absorption coefficient, [-]
A	Noise coefficient A, [dBA]
B	Noise coefficient B, [dBA]
C	Noise coefficient C, [dBA]
F	Force, [N]
i	Transmission ratio, [-]
K	Reduction noise factor, [dBA]
J	Reduction noise factor, [dBA]
l	Length, [m]
L_w	Sound power level, [dBA]
L_p	Sound pressure level, [dBA]
N	Rotational speed, [rpm]
p	Hydraulic pressure, [bar]
P	Power, [kW]
Q	Directivity factor, [-]
R	Room constant, [m ² Sabine]
r	Distance from noise source, [m]
s	Accelerator partialisation, [-]
S	Total plane surface, [m ²]
t	Time, [s]
T	Torque, [Nm]
τ	Transmission ratio, [-]
v	Vehicle speed, [km/h]
V	Displacement, [cc]
ω	Rotational speed, [rad/s]
A_1	Sun gear 1
A_2	Sun gear 2
B	Planet carrier
C	Ring gear

General subscripts

I	Hydraulic Unit I
II	Hydraulic Unit II
axle	Differential gear
ex	Engine exhaust system
h	Engine housing
hydr	Hydraulic portion
int	Engine air intake system
max	Maximum
mech,1	First full mechanical point
mech,2	Second full mechanical point
o_1	Transmission output (first gear)
o_2	Transmission output (second gear)
shift	Gear shift
tyre	Vehicle tyre
wheel	Wheel

Disclosure statement

No potential conflict of interest was reported by the authors.

ORCID

Alarico Macor  <http://orcid.org/0000-0003-2244-6524>

Antonio Rossetti  <http://orcid.org/0000-0003-0635-6748>

Martina Scamperle  <http://orcid.org/0000-0002-4822-6653>

Notes on Contributors



Alarico Macor has an MSc in mechanical engineering and a PhD in energetics from Padua University. He is associate professor of fluid power systems and teaches in the Doctoral School of Mechatronics. Research activity: Performance and emission testing of biodiesel in boilers and on-road diesel engines; Hydraulic hybrid systems and hydro-mechanical power split transmissions; dynamic simulation of fluid power systems.



Antonio Rossetti received his PhD degree in Energetic from the University of Padova, Italy, in 2009, where he held a Post-doctorate Researcher position for three years. In 2013, he moved to ITC-CNR as Researcher in the Thermo-Fluid Dynamics Branch. His main research fields are the experimental and numerical fluid dynamics.



Martina Scamperle graduated from the University of Padua in mechanical engineering in 2013. She has been a PhD student since 2014 in mechatronics and product innovation at the Department of Engineering and Management, University of Padua. Current research areas include experimental and theoretical analysis of hydrostatic transmissions, design of complex drivelines and dynamic simulation of fluid power systems

References

- AMESim, 2013. *Copyright 1996–2008, LMS imagine SA. Version 12.*
- Bies, D.A. and Hansen, C.H., 1988. *Engineering noise control: theory and practice.* London: Taylor & Francis.
- Blair, G.P. and Spechko, J.A., 1972. Sound pressure levels generated by internal combustion engine exhaust systems. SAE Technical Paper no. 720155.
- Blake, C., Ivantysynova, M., and Williams, K., 2006. Comparison of operational characteristics in power split continuously variable transmissions. *2006 SAE Commercial Vehicle Engineering Congress & Exhibition.* SAE Technical Paper no. 2006-01-3468. Rosemont, IL, USA.
- Casoli, P., et al., 2007. A numerical model for the simulation of diesel/CVT power split transmission. *ICE2007 8th International Conference on Engines for Automobiles.* SAE Technical Paper no. 2007-24-0137. Capri (NA), Italy.
- De Simio, L., Gambino, M., and Iannaccone, S., 2010. Dual fuel engines for utilization of waste vegetable oil and municipal organic fraction as energy source in urban areas. *SEEP 2010 Conference Proceedings.* Bari, Italy.
- Emission test cycle [online], 2015. Available from: <https://www.dieselnet.com/standards/cycles>
- Klop, R., Vacca, A., and Ivantysynova, M., 2009. A method of characteristics based coupled pump/line model to predict noise sources of hydrostatic transmissions. *Proceedings of the ASME Dynamic Systems and Control Conference 2009.* Volume 1, pp. 291–298. Hollywood: California.
- Klop, R. and Ivantysynova, M., 2011. Investigation of noise sources on a series hybrid transmission. *International journal of fluid power*, 12 (3), 17–30.
- Kress, J.H., 1968. Hydrostatic power-splitting transmissions for wheeled vehicles – classification and theory of operation. SAE Technical Paper no. 680549.
- Kumar Seeniraj, G. and Ivantysynova, M., 2011. A multi-parameter multi-objective approach to reduce pump noise generation. *International journal of fluid power*, 12 (1), 7–17.
- Kumar Seeniraj, G., Zhao, M., and Ivantysynova, M., 2011. Effect of combining precompression grooves, PCFV and DCFV on pump noise generation. *International journal of fluid power*, 12 (3), 53–63.
- Macor, A. and Rossetti, A., 2011. Optimization of hydro-mechanical power split transmissions. *Mechanism and machine theory*, 46 (12), 1901–1919.
- Macor, A. and Rossetti, A., 2013. Fuel consumption reduction in urban buses by using power split transmissions. *Energy conversion and management*, 71, 159–171.
- Moncada Lo Giudice, G. and Santoboni, S., 1995. *Acustica.* Milano: Ambrosiana.
- Pfiffner, R. and Guzzella, L., 2001. Optimal operation of CVT-based power trains. *International journal of robust and nonlinear control*, 11 (11), 1003–1021. Switzerland: Zürich.
- Renius, K.T. and Rainer, R., 2005. *Continuously variable tractor transmissions.* ASAE Distinguished Lecture Series. No. 29. Germany: Düsseldorf, 1–37.
- Rossetti, A. and Macor, A., 2013. Multi-objective optimization of hydro-mechanical power split transmissions. *Mechanism and machine theory*, 62, 112–128.